Spin-polarized photoemission studies of the adsorption of O and S on Fe(001)

A. Clarke
Department of Physics, Brookhaven National Laboratory, Upton, New York 11973-5000
and AT&T Bell Laboratories, Murray Hill, New Jersey 07974-2070

N. B. Brookes, P. D. Johnson, and M. Weinert
Department of Physics, Brookhaven National Laboratory, Upton, New York 11973-5000

B. Sinković* and N. V. Smith
AT&T Bell Laboratories, Murray Hill, New Jersey 07974-2070
(Received 5 January 1990)

Spin-resolved angle-resolved photoemission spectra have been measured for the adsorption systems Fe(001)-$p(1\times1)$O and Fe(001)-$c(2\times2)$S. Adsorbate-induced features in the spectra display exchange splittings (ΔE) and linewidths which vary with $k_{\parallel}$, with orbital symmetry (p_x or p_z), and with spin character. For adsorbate p_z orbitals, the measured ΔE is larger at the center of the surface Brillouin zone (1.3 eV for O, 0.5 eV for S) than at the zone boundary (0.25 and 0.2 eV, respectively). The results are compared with the predictions of tight-binding simulations and first-principles calculations.

I. INTRODUCTION

The magnetic characteristics of surfaces and thin films is currently an area of considerable research activity. This interest is a reflection of the unique properties that the lower dimensionality of these systems frequently produces.[1] Of particular interest, however, is the effect of foreign atoms or impurities adsorbed on the surface.[2-16] Such adsorption can have two principal effects: (i) a modification of the magnetic structure of the outermost atomic layers of the substrate, and (ii) a possible inducement of a magnetic moment in the adsorbate layer. Several studies concentrated on the influence of the adsorbate on the substrate magnetization. Earlier studies[2,4] of atomic oxygen and sulfur and molecular CO adsorption on nickel surfaces tended to conclude that either magnetic dead layers were formed or the magnetic moment in the surface region was reduced. In a later study[8] of oxygen and sulfur adsorption on Ni(110) and O on Fe(110) it was concluded that the adsorbate might well be polarized in the direction of the substrate and that any loss of polarization from the substrate would reflect spin-flip exchange scattering in the overlayer.

More recently attention has turned to the adsorbate itself. Several theoretical papers have concluded that for oxygen[3,7] and sulfur[13] adsorption on Fe(001) the adsorbate itself would carry a magnetic moment, $0.24\mu_B$ in the case of oxygen and $0.14\mu_B$ for sulfur. Several experimental studies[10-12] have arrived at a similar conclusion. These photoemission and inverse photoemission studies have identified exchange-split adsorbate bands which, if the bands are partially occupied, may be taken as an indication of the presence of a magnetic moment on the adsorbate.

In this paper we report further angle-resolved spin-polarized photoemission measurements on the Fe(001)-$p(1\times1)$O and Fe(001)-$c(2\times2)$ S adsorption systems, a preliminary account of this work having already appeared.[11] As reported earlier, the adsorbate-derived bands show an exchange splitting, which varies throughout the zone, in marked contrast to the results of calculations. Here we present a more extensive data set and compare these observations with both a tight-binding simulation and a new first-principles calculation. On the basis of this comparison we are able to discuss possible sources of the discrepancy between theory and experiment. We also report the observation of a spin dependence for the photoemission peak widths. These widths reflect the lifetime of the photohole and point to spin-dependent excitation effects. After outlining our experimental methods (Sec. II), we present in Sec. III a selection of typical results. Section IV is devoted to a closer analysis of the results, focusing on $E(k_{\parallel})$ dispersion relations, peak widths, and adsorbate-induced features within the substrate d band. Section V presents the results of theoretical calculations of the O/Fe system.

II. EXPERIMENTAL METHOD

The spin-polarized photoemission measurements were performed at the National Synchrotron Light Source (Upton, N.Y.) on the U5U undulator beam line. The system has been outlined previously,[11] and will be described in detail elsewhere.[17] The estimated angular resolution is $\pm1.5°$ and the estimated overall energy resolution (from both photon monochromator and electron-energy analyzer) is 0.3 eV. Spin analysis is performed by use of one of the recently developed miniature spin detectors,[18] Fig. 1.

The sample, a single-crystal Fe "picture frame" is also

shown in Fig. 1. This frame, cut with each arm along a ⟨100⟩ direction, was mounted to allow measurements with $k_{\parallel}$, the parallel components of the electron wave vector, along the $\bar{\Gamma}\bar{X}$ azimuth of the substrate surface Brillouin zone (SBZ). Spin-polarized photoemission spectra were obtained in the manner described by Kessler.[19] In order to eliminate instrumental asymmetry, the sample is first magnetized in one direction and the intensities scattered left and right (I_L^+, I_R^+) in the spin detector measured. The measurements are then repeated with the sample magnetized in the opposite direction (I_L^-, I_R^-). All measurements are made with the sample remanently magnetized. From these four measurements the polarization P, the spin-up intensity $I^{\uparrow}$, and the spin-down intensity $I^{\downarrow}$ are obtained via

$$P=\frac{1}{S}\frac{(I_L^+I_R^-)^{1/2}-(I_L^-I_R^+)^{1/2}}{(I_L^-I_R^-)^{1/2}+(I_L^-I_R^+)^{1/2}}, \tag{1}$$

$$I^{\uparrow}=\langle I\rangle(1+P), \quad I^{\downarrow}=\langle I\rangle(1-P) \tag{2}$$

where $\langle I\rangle$ is the mean of ($I_L^+, I_R^+, I_L^-, I_R^-$) and S is the Sherman function.

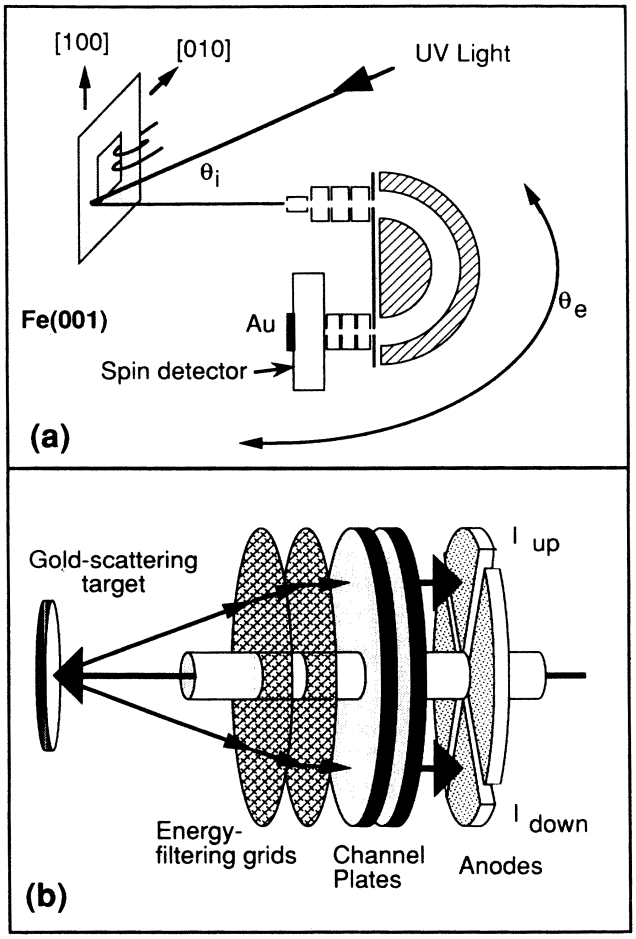

FIG. 1. (a) Schematic diagram showing the geometry and orientation of the Fe(001) picture-frame sample; light is incident at angle θ_i and electrons are collected at angle θ_e, in a plane containing the [010] azimuth ($\bar{\Gamma}\bar{X}$ direction in the surface Brillouin zone). (b) A more detailed diagram of the miniature spin detector (after Ref. 18) mounted on the exit lens of the electron-energy analyzer. Spin sensitivity is due to the spin-orbit effect in low-energy (150 eV) diffuse scattering.

Low-energy electron diffraction (LEED) and Auger-electron spectroscopy (AES) were used to monitor the surface order and cleanliness, respectively. The substrate was cleaned by repeated Ar^+-ion bombardment and annealing cycles until carbon and sulfur were undetectable with AES. At this stage further cleaning cycles removed contamination peaks from the photoemission spectra and revealed a new surface resonance feature.[20] Thereafter observation of this surface resonance was used as an indication of a clean sample. An ordered sulfur $c(2\times2)$ structure on Fe(001) was achieved by annealing the Fe substrate to 800 °C for one hour to segregate sulfur to the surface. At coverages greater than 0.5 monolayer the half-order spots were observed to split into a cluster of four spots, indicating an incommensurate overlayer. The sulfur $c(2\times2)$ system was found to be particularly inert to contamination and could be left for several hours with no significant CO contamination. Oxygen forms an ordered $p(1\times1)$ overlayer at one monolayer coverage. This was achieved by exposing the clean substrate to 6 L [1 langmuir (L) $\equiv10^{-6}$ torr for 1 sec] of O_2 and then flashing to 550 °C. Larger quantities of O_2 produce a diffuse LEED pattern with a strong background. Previous studies[21,22] of these systems indicate that for both ordered overlayers the adsorbate occupies the fourfold hollow site with the oxygen atom 0.48 Å above the surface[21] and the sulfur atom 1.0 Å from the surface.[22]

III. RESULTS

A. Non-spin-resolved data

The experimental configuration confines the electron emission direction to the mirror plane (xz) defined by the surface normal and incident-light direction. The incident light is linearly polarized in this plane. The spectra presented below will show states that are even with respect to this plane and therefore only p_x and p_z adsorbate states are observed. Figures 2(a), 2(b), and 2(c) show the spin-integrated spectra as a function of emission angle from clean Fe(001), Fe(001)-$p(1\times1)$ O, and Fe(001)-$c(2\times2)$ S, respectively. The different photon energies are indicated. A photon energy of 60 eV and emission angle of 18° corresponds to the $\bar{X}$ point in the clean and O/Fe(001) surface Brillouin zone, while a photon energy of 52 eV and emission angle of 20° corresponds again to the $\bar{X}$ point of the substrate SBZ but now the $\bar{M}$ point of the sulfur $c(2\times2)$ SBZ. Peaks in the range 4–9 eV binding energy are derived from the adsorbate $2p$ (oxygen) or $3p$ (sulfur) orbitals while emission from between 4 eV binding energy and the Fermi energy reflects the iron substrate $3d$ levels. The adsorbate-derived two-dimensional band structures obtained from Figs. 2(b) and

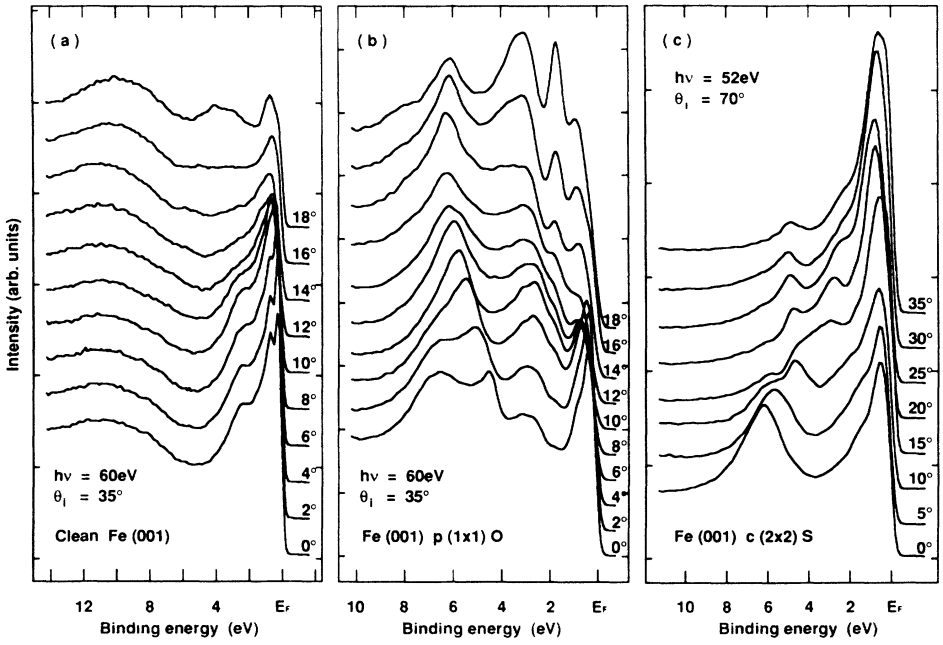

FIG. 2. Spin-integrated photoemission spectra as a function of emission angle for clean Fe(001) and for Fe(001) with ordered O and S adsorbate layers.

2(c) show close agreement with those obtained in earlier studies.[23,24]

The broad structure observed in Fig. 2(a) at a binding energy of ~ 10 eV is the Fe $M_{2,3}M_{4,5}M_{4,5}$ Auger line. It contributes a smooth background to the spectra in Fig. 2(b), but will otherwise not change the results and will not be discussed further. It does not affect the spectra of Fig. 2(c) where the photon energy of 52 eV is lower than the threshold energy for excitation of the Fe $3p$ level. However, it should be noted that at the photon energy used in the latter spectra and because of cross-section effects a sizable component of the substrate sp band appears in the peak at 6 eV binding energy near the center of the zone.

Comparing Figs. 2(a) and 2(b) it can be seen that adsorption of oxygen results in a strong modification of the Fe $3d$ bands. In particular a new feature at $\bar{X}$ and 1.7 eV binding energy is observed for oxygen exposures as low as 0.2 L. This feature and another at approximately 3 eV binding energy for normal emission have not previously been observed in studies carried out at lower photon energies. In the case of S/Fe(001) [Fig. 2(c)] there appears to be very little modification of the Fe d levels.

B. Spin-resolved data

The adsorbate-induced features are much more readily observed in the O/Fe system than the S/Fe system; a reflection of both the higher coverage and the cross-sectional dependence. Our presentation will therefore emphasize the former, but will offer comment on any differences in the behavior of the latter.

Figure 3 shows the spin-resolved normal-emission spectra obtained from Fe(001)-$p(1\times1)$ O for two angles

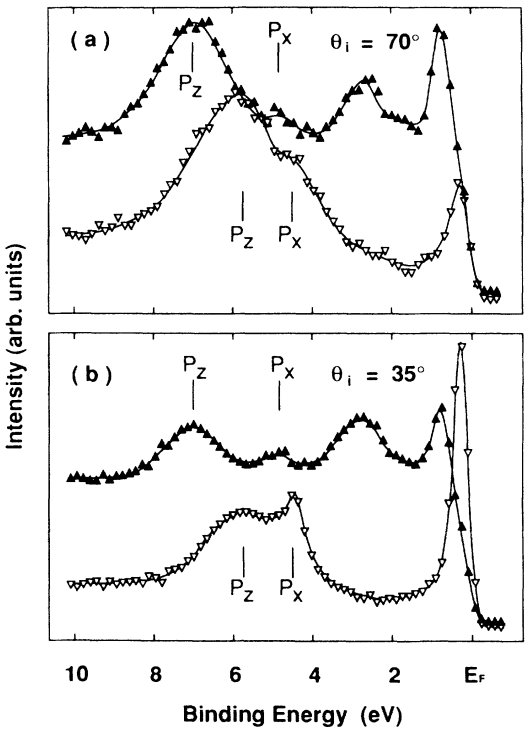

FIG. 3. Spin-resolved photoemission spectra for normal emission ($k_{\parallel}=0$) from Fe(001)-$p(1\times1)$ O. Solid upward-pointing triangles (▲) correspond to majority (↑) spin, and open downward-pointing triangles (▽) correspond to minority (↓) spin: (a) angle of light incidence $\theta_i=70°$ gives predominantly p-polarized light; (b) $\theta_i=35°$ gives larger proportion of s-polarized light. Lines are drawn to guide the eye.

of photon incidence. In Fig. 3(a), the angle of incidence of the light, $\theta_i = 70°$, gives predominantly p-polarized light and therefore favors excitation of the oxygen $2p_z$ orbital together with the Fe Δ_1 band. In Fig. 3(b), for $\theta_i = 35°$, the light contains more s polarization and both the oxygen $2p_z$ and $2p_x$ orbitals are excited. Thus varying the angle of incidence of the light allows the separate identification of the p_x and p_z orbitals in both the majority- and minority-spin spectra. Having made this assignment it can be seen that at the center of the zone the oxygen $2p_z$ peaks are exchange split by 1.3 eV while the $2p_x$ peaks are split by 0.35 eV. The minority-spin peak at 0.4 eV binding energy is assigned to the bulk $\Gamma_{25'}$ minority-spin Fe band and the majority-spin peak at 0.8 eV binding energy is assigned to the bulk Γ_{12} band. These identifications are in accord with those of earlier studies on clean Fe(001).[25] The majority-spin feature at 2.9 eV binding energy shows little sensitivity to the light polarization and we therefore believe it to be adsorbate derived. On the clean surface a majority-spin feature at similar binding energy, which is preferentially excited by s-polarized light, represents the majority component of the exchange-split $\Gamma_{25'}$ pair.

The adsorbate-derived peaks for the Fe(001)-$c(2\times2)$ S system show similar behavior to the oxygen adsorption system. Figure 4 shows the two spin components of the sulfur $3p_z$ bands, at the center of the zone, $\bar{\Gamma}$, where the exchange splitting is 0.5 eV, and at the zone boundary, $\bar{M}$, where the exchange splitting is 0.2 eV.

Some spin-resolved spectra of the O/Fe system including the Fe $3d$ region are displayed in Fig. 5 as a function of angle of emission. These show, for example, that the new feature observed in the spin-integrated spectrum at $\bar{X}$ [Fig. 2(b)] at 1.7 eV binding energy, is entirely minority-spin character. A second feature, unresolved in the spin-integrated spectra, at 2.7 eV binding energy is also found to be of minority-spin character. Both of these features persist halfway into the zone center.

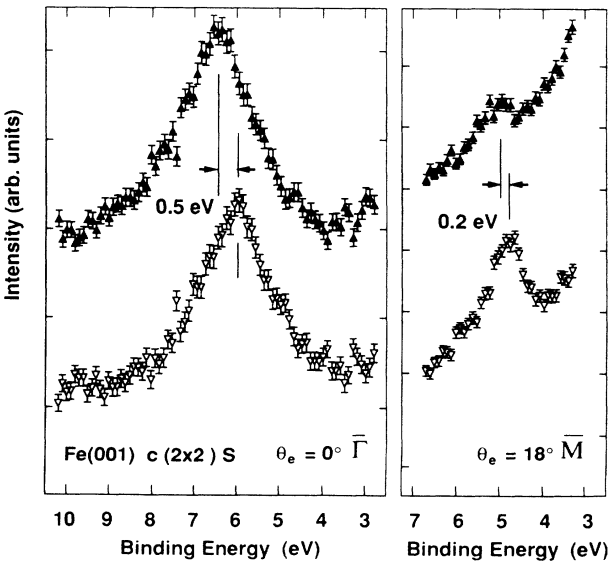

FIG. 4. Spin-resolved photoemission spectra of Fe(001)-$c(2\times2)$S at $\bar{\Gamma}$ and $\bar{M}$ ($h\nu = 52$ eV, $\theta_i = 70°$). For clarity, the energy scale is restricted to the adsorbate region. (▲ , majority spin; ▽, minority spin).

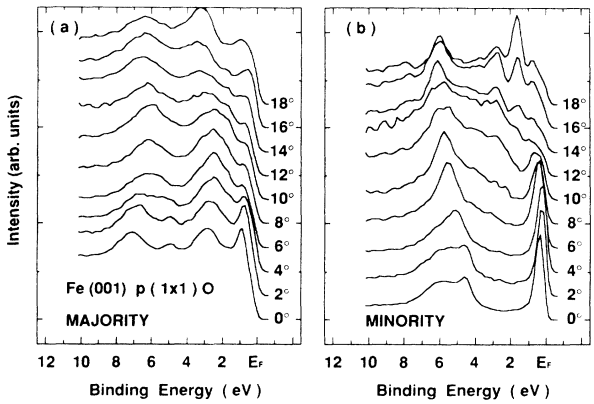

FIG. 5. Angular dependence of spin-resolved photoemission spectra from Fe(001)-$p(1\times1)$O ($h\nu = 60$ eV, $\theta_i = 35°$) corresponding to Fig. 2(b).

IV. ANALYSIS AND DISCUSSION

A. Qualitative preliminary

The obvious inference from the data in Figs. 3–5 is that the adsorbate-induced peaks for both O and S are exchange split and that the majority-spin component is more deeply bound than the corresponding minority-spin component, i.e., showing the same alignment as the substrate Fe ('3d') features. For partially filled bands it may therefore be concluded that there is an induced magnetic moment on the adsorbate atoms and that these moments are ferromagnetically aligned with each other and ferromagnetically aligned with the substrate magnetic moments. Other workers have arrived at similar conclusions.[10,12]

B. Adsorbate $E(k_\parallel)$ dispersion relations

The $E(k_\parallel)$ dispersion relations for the spin-resolved oxygen p_z and p_x orbitals for Fe(001)-$p(1\times1)$ O are shown in Fig. 6(a). The binding energies were obtained by a Gaussian line fit with an appropriate background subtraction. The data used for these fits were not broad-scan spectra such as those shown in Fig. 5, but were spectra taken over a more limited energy range with higher counting statistics. Example fits are shown in Fig. 7, which will be discussed in Sec. IV C below.

Figure 6(b) compares the observed exchange splittings with those obtained in the theoretical work of Refs. 3 and 7. The calculations predict an exchange splitting which is essentially independent of $k_\parallel$; the experimental results show a strong $k_\parallel$ dependence of the oxygen p_z exchange splitting, a discrepancy that will be discussed in what follows.

As evidenced in Fig. 4 the sulfur p_z bands also display an exchange splitting that varies throughout the zone. While the sulfur atom is displaced further from the sur-

face than the oxygen atom, 1.0 Å rather than 0.48 Å, the distance to the iron atom immediately below is only 20% larger. With the increased radius of the sulfur $3p$ orbital as compared to the oxygen $2p$ orbital it is surprising therefore that the measured exchange splitting for the sulfur p_z bands at the center of the zone is much less than that of the equivalent oxygen orbital. This may in part reflect the presence of the strong substrate sp band contribution in the sulfur spectra at this angle and energy.

C. Linewidths

We find that the linewidths of the adsorbate-induced peaks show interesting variations with orbital character, spin direction, and $k_{\parallel}$. These variations are highlighted in Fig. 7 which shows, after background subtraction, adsorbate-derived features taken in normal photoemission from Fe(001)-$p(1\times1)$O. Also shown are the results of Gaussian fits to the individual p_z and p_x orbitals. For both spin systems, the p_z-orbital peak displays a larger width than the p_x-orbital peak. Such an effect is expected on the grounds that the p_z-orbital hybridizes more strongly with substrate orbitals, as demonstrated previously both theoretically[26] and experimentally.[24]

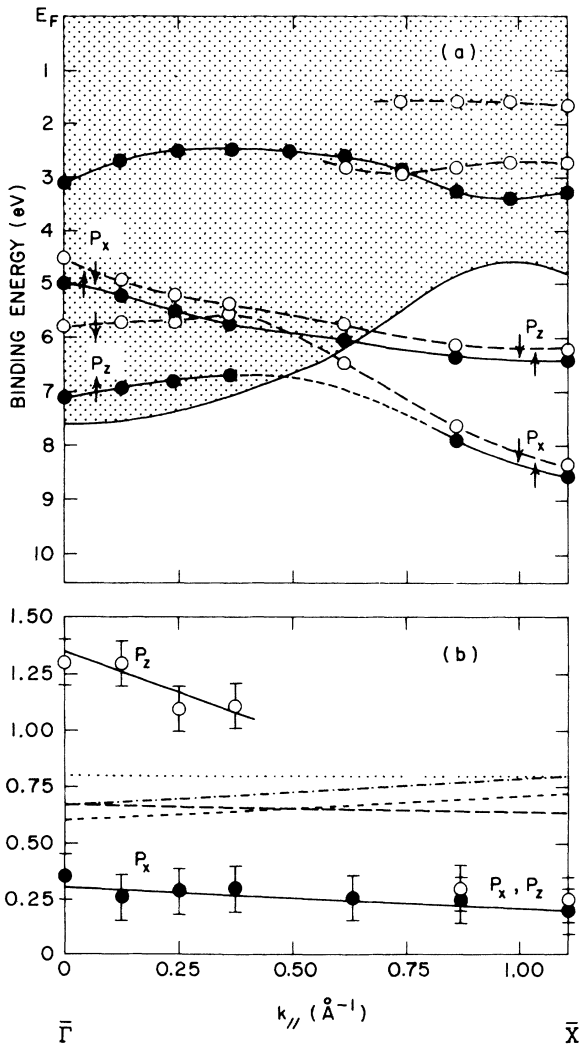

FIG. 6. (a) Spin-resolved $E(k_{\parallel})$ dispersion curves for oxygen-induced features on Fe(001)-$p(1\times1)$O; data points are given as solid (open) circles for the majority- (minority-) spin systems; the smooth curves are offered merely as a guide to the eye. (b) Comparison between the experimentally derived exchange splittings and those generated in the calculations of Ref. 3 (—·—·— and ———— for p_z and p_x, respectively) and Ref. 7 (· · · and — — —).

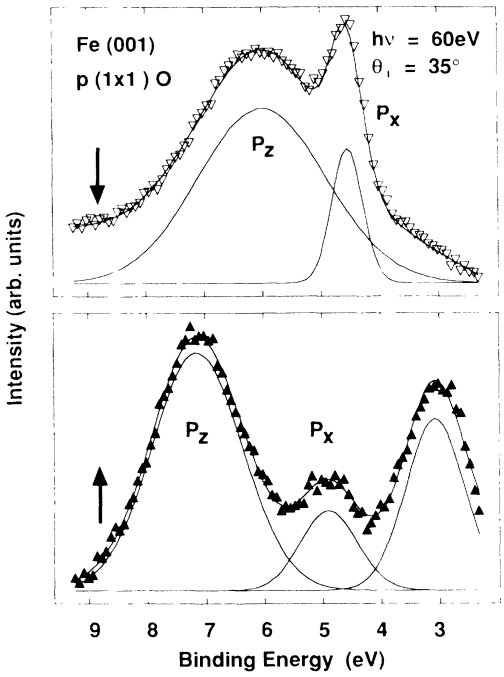

FIG. 7. Gaussian least-squares line fit to normal ($\bar{\Gamma}$) emission spectra on Fe(001)-$p(1\times1)$ O. (▲, majority spin; ▽, minority spin). The background, a simple cubic polynomial, was fitted along with the peaks.

Symmetry, on the other hand, does not allow the p_x-orbital to hybridize with the substrate at the center of the zone. Its linewidth should therefore be determined almost entirely by the lifetime of the photohole. This is explored further in Fig. 8 where the half-width (or inverse lifetime) of the p_x-orbital peak is plotted as a function of binding energy relative to E_F. Also plotted are the half-widths of the p_z-orbital peak wherever it falls outside the projected bulk continuum.

The photohole will decay primarily through Auger-like processes involving electrons at lower binding energies. Several earlier studies[27,28] of photohole lifetimes have found a linear dependence in the inverse lifetime as a function of binding energy. The present data are, however, better fitted by parabolas as shown in Fig. 8. Interestingly, in the simplest quasiparticle picture, the linewidth should vary as $(E-E_F)^2$ but only for states close to E_F. The difference between the present study and the earlier experimental studies may well reflect the fact that in the adsorbate case the photohole is relatively localized and its decay is therefore more akin to the decay of a core hole.

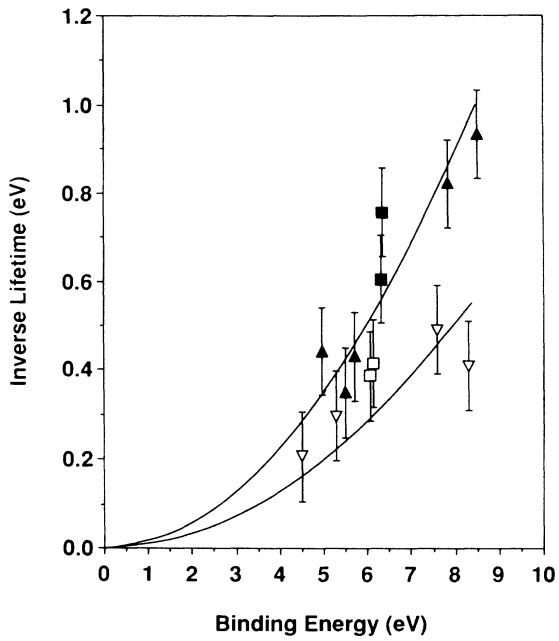

FIG. 8. Energy linewidths (or inverse lifetimes) of the oxygen-derived features typified in Fig. 7 plotted as a function of binding energy. Solid (open) triangles and squares represent the majority (minority) p_x and p_z components, respectively. The solid curves are parabolas drawn close to the majority- and minority-spin data points.

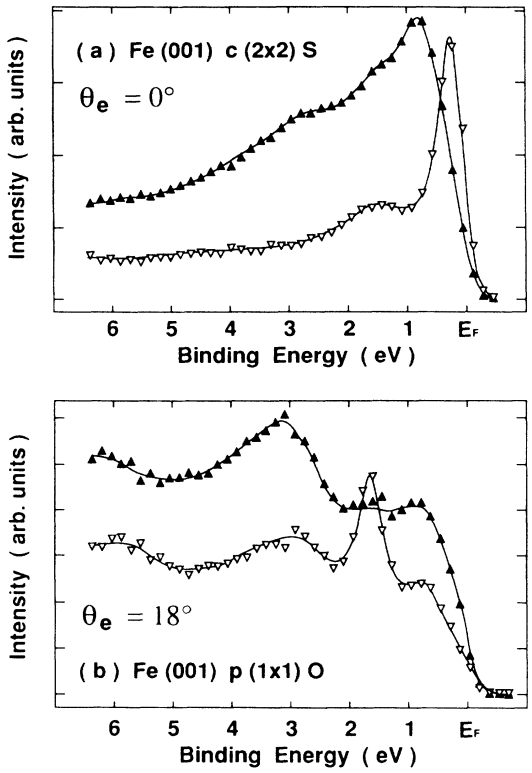

FIG. 9. Adsorbate-induced features within the Fe d band: (a) at $\bar{\Gamma}$ on Fe(001)-$c(2\times2)$ S; (b) at $\bar{X}$ on Fe(001)-$p(1\times1)$ O. (▲, majority spin; ▽, minority spin, lines are to guide the eye).

The linewidths are smaller for the minority-spin states than the majority-spin states. Indeed the relative scaling factor between the two parabolas in Fig. 8 is 1.8, close to the ratio of occupied majority-to minority-spin states for the substrate. This is consistent with the notion that the lifetime of a photohole on an adsorbed oxygen atom is determined by interatomic Auger processes in which the hole is filled by an electron of the same spin from a neighboring Fe atom.

D. Adsorbate-induced features within the Fe *d* band

So far we have focused on the adsorbate-induced peaks which occur below the Fe d-band manifold. Adsorbate-induced peaks appear also within the Fe d-band. These are already indicated in Fig. 6 which shows the $E(k_{\parallel})$ dispersion relations for a number of features in the energy range 1.5–3.5 eV below E_F. The experimental data used for these plots are exemplified in Fig. 9, which shows spin-resolved photoemission spectra at $\bar{\Gamma}$ for Fe(001)-$c(2\times2)$S and at $\bar{X}$ for Fe(001)-$p(1\times1)$O. The S-adsorption data will not be analyzed further here, but are offered as an illustration of how spin-detection can reveal adsorbate-induced features (in this case the weak minority-spin peak at 1.4 eV) not apparent in the spin-integrated spectra. The O-adsorption data exhibit three noteworthy features. The strong peak at 1.7 eV seen in spin-integrated spectra is, as already mentioned, of entirely minority-spin character. At approximately 3 eV there is in clean Fe(001) [see Fig. 2(a)] a feature which becomes significantly enhanced on O adsorption [see Fig. 2(b)]. The spin-resolved spectra of Fig. 9 show that most of this enhancement occurs in the majority-spin system (the adsorbate-induced peak occurring at 3.2 eV) but reveal also a weak adsorbate-induced feature at 2.8 eV in the minority-spin system. These three features (at 1.7, 2.8, and 3.2 eV at $\bar{X}$) and their dispersions away from $\bar{X}$ have been plotted in Fig. 6(a). The theoretical origin of these features will be presented in Sec. V B.

V. THEORETICAL COMPARISONS

To gain some insight into the experimental results, we have performed two kinds of theoretical calculation: tight-binding simulations and first-principles slab computations. These are now discussed.

A. Tight-binding simulations

It was shown some time ago[26] that first-principles calculations of $E(k_{\parallel})$ dispersion relations for O adsorbed on Ni(001) can be made intelligible in terms of a tight-binding-like $E(k_{\parallel})$ band structure for an isolated O monolayer distorted by hybridization with the orbitals of the metal substrate. We have therefore set up a tight-binding simulation to investigate what happens when the substrate band structure is spin split.

The tight-binding parameters for the isolated O overlayer were obtained by first fitting to the results of Liebsch,[26] and then scaling to the new O-O lattice param-

eter appropriate to Fe(001)-$p(1\times1)$O according to the recipes set forth in the book by Harrison.[29] The results of this procedure are shown as the $E(k_{\parallel})$ plot of Fig. 10(a). To model the adsorption system the bulk Fe-Fe parameters were two center nonorthogonal parameters taken without modification from the book by Papaconstantopoulos;[30] the Fe-O parameters were obtained from Harrison.[29]

The main effects of switching on the Fe-O interactions was to lower the mean energy of the O p-orbital manifold, to broaden its energy width, and to convert the crossing of the p_z and p_x bands into an avoided crossing. All these features are in agreement with experiment and are achieved with no parameter adjustment. The downward shifts are different in the spin-up and spin-down manifolds, bringing about an exchange splitting of the O p-states. This is readily understood in terms of second-order perturbation theory in which the respective energy shifts would be $|h_{pd}|^2/(E_{d\uparrow}-E_p)$ and $|h_{pd}|^2/(E_{d\downarrow}-E_p)$ where h_{pd} is the appropriate hybridization matrix element, and $E_{d\uparrow}$, $E_{d\downarrow}$, and E_p are the unperturbed substrate d and adsorbate p energies. Since $E_{d\uparrow}$ and $E_{d\downarrow}$ are nondegenerate ($\Delta E_{ex}\sim2.2$eV) the energy shifts will differ. This differential hybridization shift results in the exchange splitting of the O p levels and since a part of the hybridized d states crosses the Fermi energy also results in an associated small magnetic moment on the adsorbate.

The particular simulation of Fig. 10(b) has been contrived to reproduce the exceptionally large exchange splitting for the O p_z orbitals at $\bar{\Gamma}$. This is achieved by noting that at $\bar{\Gamma}$ the principal adsorbate-substrate interactions are between the O p_z orbital and the d_{z^2} orbital on the Fe atom directly below in the Fe second layer (σ bonding), and between the O p_x orbital and the first layer Fe d_{xz} orbital (π bonding). The main effects of simply increasing the $p_z-d_{z^2}$ ($pd\sigma$) interaction with the Fe atom directly below the oxygen are to increase the p_z exchange splitting uniformly across the zone and to shift the p_z bands to deeper binding energies. The simulation in Fig. 10(b), however, is achieved by reducing the σ interactions; by a factor of approximately 2 for the $pp\sigma$ interactions and a factor of 6 for the $pd\sigma$ interactions. The π interactions were left unchanged except for $pd\pi$ between the oxygen and the Fe atom directly below, which was increased by a factor of 3.5. Unfortunately, the intuitively appealing insight provided by such modeling does not survive in first-principles calculations. (See Refs. 3 and 7 and Sec. V B immediately below.) It should be emphasized, however, that our original (i.e., uncontrived) sets of tight-binding parameters gave $k_{\parallel}$-independent exchange splittings in accord with the first-principles results.

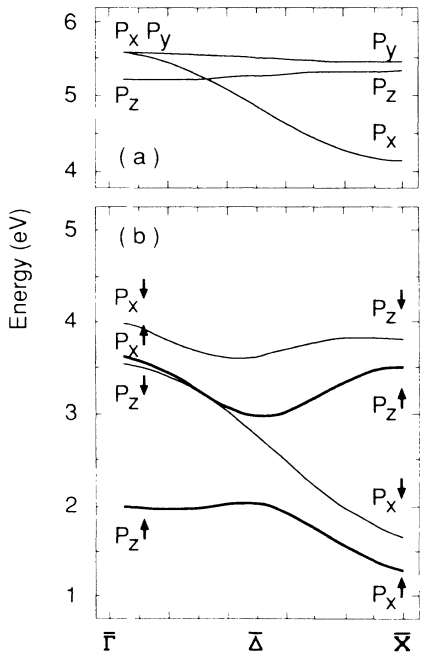

FIG. 10. Tight-binding simulations of the two-dimensional band structure of (a) an isolated layer of O atoms, and (b) the same layer hybridizing with a spin-split Fe substrate.

B. First-principles results

We have also performed first-principles calculations for Fe(001)-$p(1\times1)$O using the full-potential linear augmented-plane-wave (FLAPW) method.[31] The configuration was a 49-layer O/Fe(001) slab with atoms in the positions known from LEED analysis.[21] The potential and density for this thick film were obtained by a stretching technique that makes use of thinner slab and bulk results. Although the calculations are not self-consistent enough for total energy purposes the bands are stable. The results of these calculations for the $E(k_{\parallel})$ dispersion relations are shown in Fig. 11, and should be compared with the corresponding experimental data shown in Fig. 6.

A significant advantage of such thick films is that the bulk projected bands and gaps are obvious. The majority-spin and minority-spin projected bands show important differences in width and overlap: the two lowest majority-spin bulk bands are both narrower and overlap each other more than the corresponding minority states.

The oxygen p_x and p_z orbitals discussed above are seen below about 3.5 eV. These states are true surface states near $\bar{X}$ and are extremely localized around the oxygen. The O p_x level is again well localized at $\bar{\Gamma}$, but between the where the level crosses the bulk continuum and $\bar{\Gamma}$, the orbital becomes more delocalized. This type of delocalization due to hybridization with the substrate is even more obvious in the case of the O p_z orbital. As the adsorbate orbital crosses the bulk continuum it becomes a resonance with its spectral weight spread out over an energy range of ~0.5 eV, consistent with the increased linewidth seen experimentally and found in earlier calculations.[26] Further, in agreement with previous theoretical calculations[3,7] we find an exchange splitting of these predominantly oxygen-derived states which remains

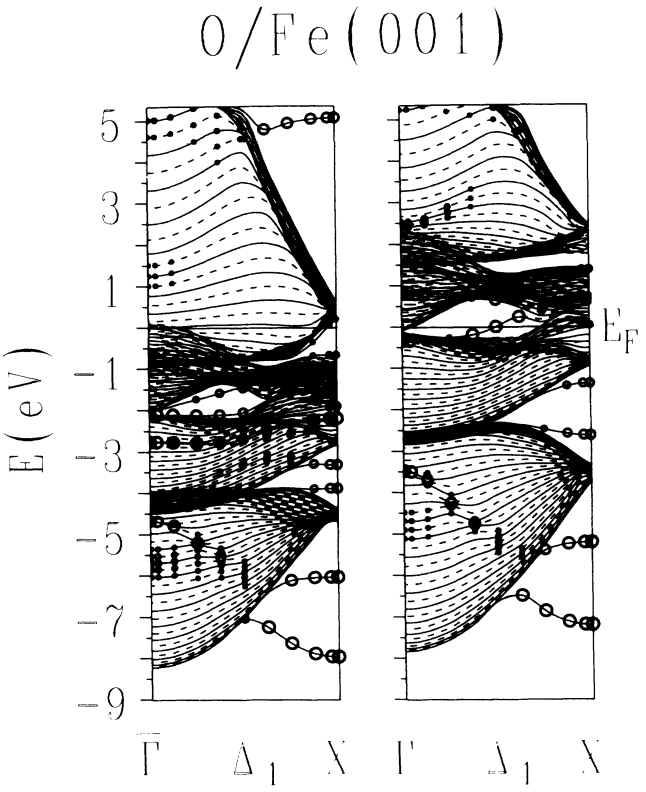

FIG. 11. First-principles 49-layer slab calculation of the $E(k_\parallel)$ dispersion relations for the adsorption system Fe(001)-$p(1\times1)$O for states of $\bar{\Delta}_1$ symmetry. Surface states are marked with circles whose size increases with increased localization in the surface region. The diagram on the left shows states of majority-spin character, the right minority-spin character.

essentially independent of $k_\parallel$ and is significantly too large. (The p_x exchange splitting at $\bar{\Gamma}$ does increase, due mainly to the majority-spin member being forced to greater binding energy reflecting level repulsion with the surface resonance at 2.8 eV.) A possible explanation of this behavior will be discussed below.

Above 3.5 eV at $\bar{X}$ there is a prominent projected gap in the minority-spin system which supports two surface states at 1.4 and 2.6 eV. These are readily identifiable with experimentally observed minority states at 1.7 and 2.8 eV discussed above in Sec. IV D and displayed in Figs. 6(a) and 9(b). The state at the bottom of the gap reflects the bonding of the adsorbate p_z orbital with an existing Fe(001) surface state,[20] that at the top of the gap reflects the bonding of the adsorbate p_x orbital with Fe states at the top of the gap. Similar oxygen-derived states are observed in the corresponding majority-spin gap of the calculation at 3.3 and 3.9 eV. These are identifiable with the broad structure seen in the experiment centered at 3.2 eV, Fig. 9(b). At $\bar{\Gamma}$, there is a majority surface resonance at 2.8 eV which is strong and which extends well out towards $\bar{X}$. There appears to be no counterpart of this feature in the minority-spin system in either theory or experiment. We identify the majority feature between 2.5 and 3.5 eV plotted in Fig. 6(a) with this theoretical resonance. As it approaches $\bar{X}$, it merges with the gap states, a result which we attribute to imperfect angular and energy resolution.

C. Concluding comments

The overall conclusion of this paper is that spin-polarized photoemission studies reveal an exchange splitting for adsorbates on a ferromagnetic substrate, and that $E(k_\parallel)$ dispersion relations are in fair agreement with available theoretical calculations. There remain some discrepancies. The quantitative magnitudes of the adsorbate exchange splitting and its $k_\parallel$ dependence are not well reproduced by theory. Such a discrepancy may reflect excitation effects in that the experiment samples the spectral properties of the excited state, the calculation represents the ground state. Indeed a marked difference in the linewidth of spin-up and spin-down adsorbate features has been observed. Energy shifts and energy linewidths may be regarded, respectively, as the real and imaginary parts of a self-energy due to many-body dynamical effects. However, in the absence of any detailed calculation it is unclear as to how large an effect this represents. We therefore propose this as a topic worthy of further study. Another possible source of the discrepancy may be inherent in the calculation itself, i.e., the use of the local-spin-density approximation (LSDA) to the exchange-correlation potential. In the LSDA, all spin effects are included via an effective local magnetic field $B(\mathbf{r})$ that acts on all states of a given spin regardless of their orbital character. For homogeneous magnetic systems such as elemental Fe, this is not an unreasonable assumption since all states that are participating in the magnetization are of similar orbital character. For an adsorbate system, however, the orbital character of the adsorbate and substrate are different and the LSDA assumption may be inappropriate. For example, even if the symmetries of the adsorbate and substrate did not allow any interaction, there would still be an induced adsorbate exchange splitting resulting from the effect of the LSDA $B(\mathbf{r})$. For an oxygen p orbital in the O/Fe(001) calculation, this effect is estimated to be of the order of 0.6 eV. Adsorbate states that do not hybridize so much with the substrate (O p_x throughout the zone and p_z below the bulk continuum) would be expected to have an approximately large and constant exchange splitting independent of $k_\parallel$. For heavily hybridized substrate-adsorbate states, the error will be decreased since it is proportional to the oxygen contribution to the wave function. Thus for the O p_z orbital which interacts strongly with many Fe bands (the wide resonance seen in Fig. 11), the error in the exchange splitting should be less. Using these arguments to correct the calculated exchange splitting would give answers in reasonable agreement with the experimental results of Fig. 6. These results are also consistent with the tight-binding calculations. The effect of the LSDA $B(\mathbf{r})$ term is to strongly couple the adsorbate orbital to

the exchange splitting of the substrate, which in a tight-binding method can be corrected by a reduction of the attractive h_{pd} matrix elements. Although this clarifies the origin of the error in the adsorbate exchange splittings using the LSDA, it unfortunately does not provide a formally consistent method to include these types of exchange interactions into first-principles calculations. More work on this topic will be needed before one can completely reconcile theory and experiment.

ACKNOWLEDGMENTS

We are indebted to Professor A. Arrott and S. D. Bader for the loan of the Fe picture-frame sample. We have profited from discussions on spin polarimetry with R. J. Celotta and D. T. Pierce. This work was supported in part by the U. S. Department of Energy under Contract No. DE-AC02-76-CH00016 and the National Science Foundation under Contract No. DMR-86-03304.

*Present address: NYU, Department of Physics, New York, N.Y. 10003.

[1]A. J. Freeman, C. L. Fu, S. Ohnishi, and M. Weinert, in *Polarized Electrons in Surface Physics,* edited by R. Feder (World Scientific, Singapore, 1985).

[2]W. Schmitt, H. Hopster, and G. Güntherodt, Phys. Rev. B **31**, 4035 (1985).

[3]H. Huang and J. Hermanson, Phys. Rev. B **32**, 6312 (1985).

[4]A. Seiler, C. S. Feigerle, J. L. Pena, R. J. Celotta, and D. T. Pierce, J. Appl. Phys. **57**, 3638 (1985); Phys. Rev. B **32**, 7776 (1985).

[5]R. Allenpach, M. Taborelli, and M. Landolt, Phys. Rev. Lett. **55**, 2599 (1986).

[6]C. S. Feigerle, A. Seiler, J. L. Pena, R. J. Celotta, and D. T. Pierce, Phys. Rev. Lett. **56**, 2207 (1986).

[7]S. R. Chubb and W. E. Pickett, Phys. Rev. Lett. **58**, 1248 (1987).

[8]W. Schmitt, K. -P. Kämper, and G. Güntherodt, Phys. Rev. B **36**, 3763 (1987).

[9]L. E. Klebanoff, R. K. Jones, D. T. Pierce, and R. J. Celotta, Phys. Rev. B **36**, 7849 (1987).

[10]G. Schönhense, M. Donath, U. Kolac, and V. Dose, Surf. Sci. **206**, L888 (1988).

[11]P. D. Johnson, A. Clarke, N. B. Brookes, S. L. Hulbert, B. Sinković, and N. V. Smith, Phys. Rev. Lett. **61**, 2257 (1988).

[12]G. Schönhense, M. Getzlaff, C. Westphal, B. Heidemann, and J. Bansmann, J. Phys. (Paris) Colloq. **8**, C-1643 (1988).

[13]S. R. Chubb and W. E. Pickett, Phys. Rev. B **38**, 10 227 (1988); **38**, 12 700 (1988); J. Appl. Phys. **63**, 3493 (1988).

[14]B. Sinković, P. D. Johnson, N. B. Brookes, A. Clarke, and N. V. Smith, Phys. Rev. Lett. **62**, 2740 (1989).

[15]N. B. Brookes, A. Clarke, and P. D. Johnson, Phys. Rev. Lett. **63**, 2764 (1989).

[16]P. D. Johnson, J. Electron Spectrosc. Relat. Phenom. (to be published).

[17]P. D. Johnson, S. L. Hulbert, R. Klaffky, N. B. Brookes, A. Clarke, B. Sinković, M. J. Kelley, and N. V. Smith (unpublished).

[18]J. Unguris, D. T. Pierce, and R. J. Celotta, Rev. Sci. Instrum. **57**, 1314 (1986).

[19]J. Kessler, *Polarized Electrons,* Vol. 1 of *Springer Series on Atoms and Plasmas* (Springer-Verlag, Berlin, 1985).

[20]N. B. Brookes, A. Clarke, P. D. Johnson, and M. Weinert, Phys. Rev. B **41**, 2643 (1990).

[21]K. O. Legg, F. Jona, D. W. Jepsen, and P. M. Marcus, Phys. Rev. B **16**, 5271 (1977).

[22]K. O. Legg, F. Jona, D. W. Jepsen, and P. M. Marcus, Surf. Sci. **66**, 25 (1977).

[23]G. Panzner, D. R. Mueller, and T. N. Rhodin, Phys. Rev. B **32**, 3427 (1985).

[24]R. A. Didio, E. W. Plummer, and W. R. Graham, Phys. Rev. Lett. **52**, 683 (1984).

[25]E. Kisker, K. Schröder, W. Gudat, and M. Campagna, Phys. Rev. B **31**, 329 (1985).

[26]A. Liebsch, Phys. Rev. B **17**, 1653 (1978).

[27]J. A. Knapp, F. J. Himpsel, and D. E. Eastman, Phys. Rev. B **19**, 4952 (1979).

[28]S. D. Kevan and D. A. Shirley, Phys. Rev. B **22**, 542 (1980).

[29]W. A. Harrison, *Electronic Structure and the Properties of Solids* (Freeman, San Francisco, 1980).

[30]D. Papaconstantopoulos, *Handbook on the Band Structure of Elemental Solids* (Plenum, New York, 1986).

[31]E. Wimmer, H. Krakauer, M. Weinert, and A. J. Freeman, Phys. Rev. B **24**, 864 (1981).

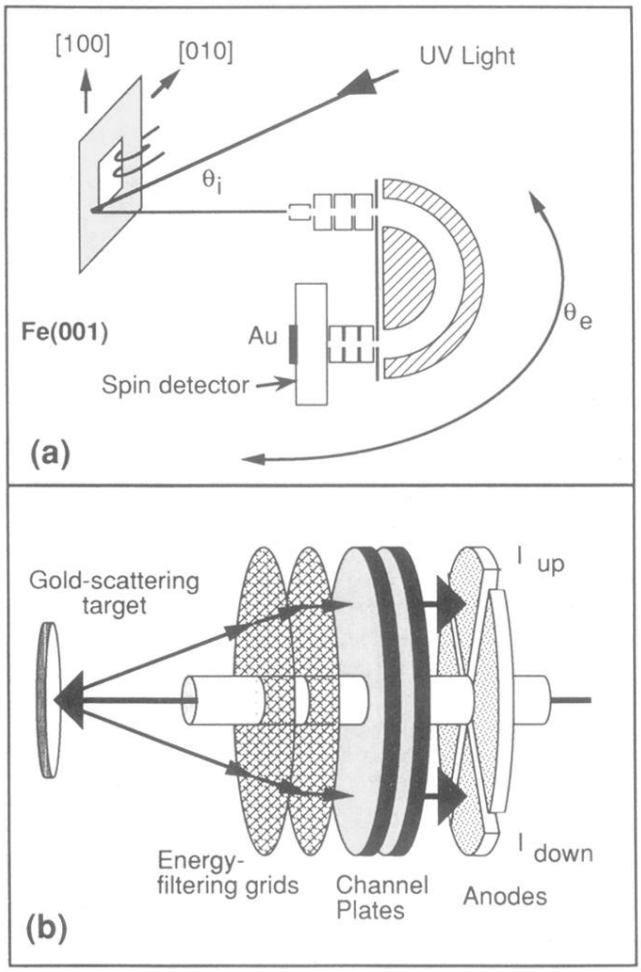

FIG. 1. (a) Schematic diagram showing the geometry and orientation of the Fe(001) picture-frame sample; light is incident at angle θ_i and electrons are collected at angle θ_e, in a plane containing the [010] azimuth ($\bar{\Gamma}\bar{X}$ direction in the surface Brillouin zone). (b) A more detailed diagram of the miniature spin detector (after Ref. 18) mounted on the exit lens of the electron-energy analyzer. Spin sensitivity is due to the spin-orbit effect in low-energy (150 eV) diffuse scattering.